ACS OMEGA

Open Access

This article is licensed under CC-BY-NC-ND 4.0

http://pubs.acs.org/journal/acsodf

Article

Accelerated Water Desorption of Oligomeric Poly(ethylene glycol) by Addition of Poly(propylene glycol) for Energy-Efficient Water Recovery Systems

Daisuke Ikegawa, Arisa Fukatsu,* Kenji Okada, and Masahide Takahashi*

Cite This: *ACS Omega* 2024, 9, 1084−1091

Read Online

ACCESS | Metrics & More | Article Recommendations | Supporting Information

ABSTRACT: Adsorbents are used to recover water vapor from the atmosphere in desiccant air conditioning (DAC) and atmospheric water harvesting (AWH) systems. Solid adsorbents have been conventionally used in these systems, though liquid adsorbents are considered to be more effective for energy-efficient fluidic thermosystems because of their low regeneration temperatures (45−70 °C). While most previous studies have focused on improving the adsorption performance, the desorption performance of adsorbents can also be a critical factor in improving the energy efficiency of these systems. Thus, this study aimed to improve the water desorption efficiency, focusing on the liquid adsorbents. We found that mixing hydrophobic molecules into a liquid adsorbent decreases the desorption temperature and increases the water-desorption efficiency. Oligomeric poly(ethylene glycol) (PEG), a common moisture-adsorbing liquid oligomer used in detergents and cosmetics, was selected as the liquid adsorbent. Oligomeric poly(propylene glycol) (PPG), which has a structure analogous to PEG and lower hygroscopicity, was selected as the hydrophobic molecule. Water adsorption and desorption experiments showed that the mixture of PPG with PEG promoted the desorption of water molecules beyond that of PEG, while thermogravimetric differential thermal analysis revealed a decrease in the water desorption temperature with increasing PPG content. The improved desorption efficiency was ascribed to the likely water adsorption equilibrium between PEG and PPG in the blend; water molecules are preferentially desorbed from PPG, which has weaker water−adsorbate interactions. The proposed concept is expected to be incorporated into various hygroscopic liquids to develop energy-efficient liquid adsorbents for DAC and AWH.

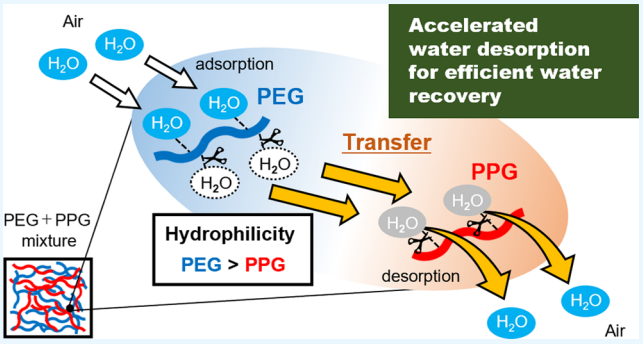

INTRODUCTION

Global population growth has been accompanied by an increase in energy demand, which is predicted to be 48% over the next 20 years.[1] This has made efficient energy use an important research topic. Abundant and ubiquitous waste energies that can be efficiently exploited for "low-grade heat" to address the energy demand question include industrial waste gases, solar power, and geothermal heat.[2] However, because of the low temperatures, technologies for the regenerative extraction of low-grade heat are currently limited,[3] and many industrial processes waste these potential energy sources.[4] The effective utilization of low-grade heat promises to contribute to achieving energy sustainability.[5] A wide range of technologies are currently being developed to utilize low-grade heat in air conditioning, power generation,[6] agricultural processes,[7] and water systems.[8] There has been particular interest in the development of adsorbents for desiccant air conditioning (DAC)[9] and atmospheric water harvesting (AWH)[10] systems, which enable the recovery of water vapor from the air under low humidity conditions in an energy-efficient manner. In these systems, it is important to develop adsorbents that can be regenerated using low-grade heat to achieve autonomous DAC and AWH. Solid and liquid adsorbents exist, among which liquid adsorbents are expected to be effective targets for low-grade heat because they can achieve a lower regeneration temperature than solid adsorbents and are favorable for flexible system design because of their flowability.[11]

An ideal liquid adsorbent must exhibit good adsorption and desorption performances. Previous studies have mainly used metal-salt solutions[12,13] and ionic liquids.[14] Most previous studies have focused on improving the adsorption performance. Ionic liquids have attracted particular attention because their physicochemical properties can be tuned by selecting appropriate cations and anions. Among the currently reported ionic liquids for water adsorption, 1-ethyl-3-methylimidazo-

Received: September 22, 2023
Revised: November 30, 2023
Accepted: December 1, 2023
Published: December 18, 2023

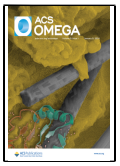

ACS Publications

© 2023 The Authors. Published by American Chemical Society

https://doi.org/10.1021/acsomega.3c07310
ACS Omega 2024, 9, 1084−1091

lium acetate ([EMIM][Ac]) is one of the most promising candidates because it can bind water molecules with high binding energy and provide a large water adsorption capacity.[14] This indicates that [EMIM][Ac] is an excellent adsorbent, but at the same time, it requires a large amount of energy to desorb water molecules. Therefore, the use of more energy-efficient adsorbents requires innovative schemes to facilitate the desorption of adsorbed water molecules. A study by Che et al. on DAC applications focused on improving desorption performance.[12] They reported that mixing a metal-salt solution with superior desorption performance improved the desorption performance of the adsorbent and lowered the regeneration temperature by 4 K. They also reported a 40% improvement in the energy utilization efficiency of the system owing to a lower regeneration temperature. This shows that improving the desorption performance of liquid adsorbents is important because it improves the energy utilization efficiency. However, the ionic liquids and metal-salt solutions used in previous studies are not practical because ionic liquids are expensive and metal-salt solutions require maintenance owing to the evaporation of water from the solution and the solution's corrosiveness. Therefore, practical liquid adsorbents must combine the characteristics of low cost, noncorrosiveness, and excellent adsorption and desorption performance.

In this study, we propose a new concept to improve the desorption efficiency of adsorbed water molecules for practical liquid adsorbents with a high energy utilization efficiency. Specifically, we attempted to increase the desorption efficiency by mixing less hydrophilic molecules with a liquid adsorbent for the desorption of adsorbed water molecules. Oligomeric poly(ethylene glycol) (PEG), a common liquid compound used in detergents and cosmetics—known for its ability to adsorb water molecules even at low humidity, was selected as the liquid adsorbent. Poly(propylene glycol) (PPG), which has a similar structure and lower hygroscopicity compared to PEG, was selected as the hydrophobic additive. Liquid PEG and PPG were mixed in different ratios to investigate their water desorption capacities.

EXPERIMENTAL SECTION

Materials. Poly(ethylene glycol) 300 (average molecular weight: 260−340, liquid at room temperature), poly(propylene glycol) 400 (average molecular weight: 400, liquid at room temperature), poly(propylene glycol) 4000 (average molecular weight: 4000, liquid at room temperature), and potassium carbonate (99.5%) were purchased from FUJIFILM Wako Pure Chemical Corporation. All reagents were used without further purification. Water was purified by using Direct-Q UV3 (Millipore).

Equipment. The humidity and temperature in the incubator were monitored using an Ondotori RTR 507B (T&D Corporation) thermo-hygrometer. Thermogravimetric differential thermal analysis (TG-DTA) was performed using a Thermo plus EVO (Rigaku) equipment. Attenuated total reflection Fourier-transform infrared (ATR FT-IR) spectroscopy was performed using an ALPHA (Bruker) spectrometer.

Establishment of a Constant Temperature and Humidity Environment. Arbitrary humidity was prepared by a saturated salt method based on the Japanese Industrial Standards (JIS Z 8806). The relative humidity of air in equilibrium with a saturated aqueous salt solution depends on the salt and the temperature of the solution. The saturated salt method uses this property to generate an arbitrary humidity. In this study, a saturated aqueous potassium carbonate solution was placed in an incubator and an arbitrary humidity was generated. A thermo-hygrometer was used to monitor the humidity and temperature in the incubator. The incubator containing the saturated potassium carbonate solution was kept constant at 30−40% relative humidity (RH) and 25 °C or 20%RH and 40 °C. The effect of humidity on water adsorption and desorption of the samples was investigated by varying the humidity conditions under which the samples were maintained. (See Figure S1 for details.)

Water Adsorption and Desorption Experiment. All experiments were performed under constant temperature and humidity, controlled using the setup described above. Adsorbent samples of 0.5 g were placed in an incubator with constant humidity at 30%RH and 25 °C and allowed to stand for 2 days to adsorb water. The water-adsorbed samples were then dehydrated in an incubator at 20%RH and 40 °C. The mass of each sample was measured by using an electronic balance before and after it was placed in an incubator maintained at an arbitrary humidity level. The experimental procedure used is illustrated by a flowchart in Figure S2. Water adsorption of the sample was determined by measuring the mass of the sample before and after it was placed in an incubator at an arbitrary humidity. The mass of the water-adsorbed sample was measured before and after heating, and the change in mass before and after heating was used as the water desorption volume of the sample. The amount of water in the sample, W_w, was determined using eq 1

$$W_w = (M_s - M_s^\circ)/M_s^\circ \quad (1)$$

where M_s is the weight of the sample and M_s° is the initial weight of the sample. The amounts of water adsorbed and desorbed from the sample were evaluated from W_w.

Material Characterization. The endothermic temperature due to water desorption during heating was measured by a thermogravimetry-differential thermal analyzer in the range from room temperature to 150 °C. The rate of increase was set at 7 °C/min. Infrared (IR) spectra were obtained for the droplet on a single reflection attenuated total reflection (ATR) module of Fourier-transform infrared (FT-IR) spectrometer in the 500−3800 cm^{-1} range. All spectra were normalized by C−O−C stretching bands at 1058−1090 cm^{-1}.

RESULTS AND DISCUSSION

Evaluation of Water Adsorption Capacity of Adsorbents. PEG300 and PPG400 were mixed in various ratios, and water adsorption tests were performed to quantitatively evaluate the water adsorption capacity of each sample. Notably, all of the mixtures were miscible, and the experiments were performed with homogeneous mixtures. ATR FT-IR spectroscopy was used to evaluate the samples before and after water adsorption. In the ATR FT-IR spectra of PEG300 (Figure S3) and PPG400 (Figure S4), the evident increase in the intensity of the peaks attributed to water molecules (−OH stretching mode (3400 cm^{-1}) and H−O−H bending mode (1650 cm^{-1}))[15] strongly indicated that both adsorbents had adsorbed water molecules from the atmosphere at 30%RH and 25 °C. Under these conditions, PEG300 and PPG400 exhibited water adsorption capacities of 8 and 2 wt %, respectively (Figure 1).

For the mixtures of PEG300 and PPG400, the total water adsorption capacity decreased as the weight percentage of PPG400 increased. This is due to the difference in the

https://doi.org/10.1021/acsomega.3c07310
ACS Omega 2024, 9, 1084−1091

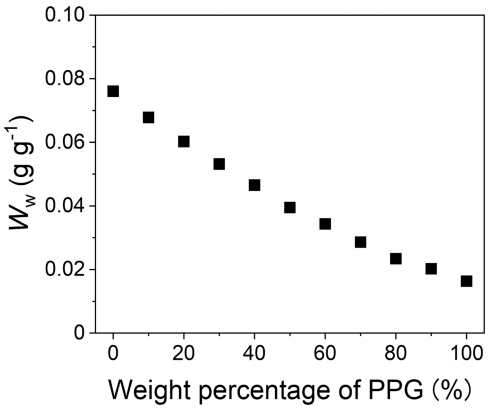

Figure 1. Water contents of PEG300 and PPG400 mixtures, W_w, as a function of the weight percentage of PPG400 (0, 10, 20, 30, 40, 50, 60, 70, 80, 90, or 100%) in the water-adsorption experiments at 30% RH and 25 °C for 2 days.

adsorption capacities of more hydrophilic PEG300 and less hydrophilic PPG400. Because the decrease in the adsorption capacity followed the additivity rule, it was found that the incorporation of PPG400 did not affect the adsorption capacity of PEG300.

Evaluation of Water Desorption Capacity of Adsorbents. Water desorption tests were performed to confirm the effect of blending PPG400 on the water desorption of the adsorbents. Water was adsorbed until the samples reached an equilibrium adsorption state at 30%RH and 25 °C and desorbed at 20%RH and 40 °C until the samples reached equilibrium. These temperatures virtually represent an average ambient atmosphere in the arid region, such as the Arabian Desert (30%RH and 25 °C)[16] and the use of low-grade heat from sunlight during the day (20%RH and 40 °C). The water recovery rate of the samples was evaluated using an index called water desorption efficiency, η_{des}, as shown in eq 2

$$\eta_{des} = W_{des}/W_{ads} \quad (2)$$

where W_{des} is the amount of water desorbed and W_{ads} is the amount of water adsorbed.

Figure 2 shows the relationship between the weight percentage of PPG400 and the water-desorption efficiency.

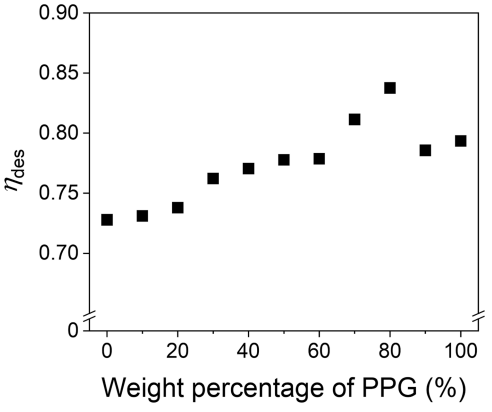

Figure 2. Water desorption efficiencies of PEG300 and PPG400 mixtures, η_{des}, as a function of the weight percentage of PPG400 (0, 10, 20, 30, 40, 50, 60, 70, 80, 90, or 100%) in the water-adsorption (30%RH and 25 °C for 2 days) and water-desorption (20%RH and 40 °C for 2 days) experiments.

Evidently, the larger the weight percentage of PPG400, the higher the water desorption efficiency. The value of the water desorption efficiency was the maximum at 80 wt % of PPG400. As the weight percentage of PPG400 reached 70−80 wt %, PEG300 and PPG400 mixtures showed higher water desorption efficiency than PPG400 alone. This indicates that PEG300 and PPG400 interact with each other and exhibit enhanced desorption of the adsorbed water molecules.

The desorption kinetics were analyzed for mixtures of PEG300 and PPG400 in various ratios. Before the experiments, the mixtures were kept in an incubator at 30%RH and 25 °C until the water adsorption reached equilibrium. The water-saturated mixtures were then placed at 20%RH and 40 °C to evaluate the desorption kinetics. It should be noted here that the desorption experiments were performed under mild conditions (20%RH and 40 °C). The weight change during water desorption was normalized by the amount of the water adsorbed at equilibrium under 30%RH at 25 °C, and the water desorption rate of the sample was evaluated as the normalized water content, nW_w. The relationship between time and nW_w for the PEG300 and PPG400 mixtures showed a negative linear slope (Figure S5). Therefore, the water desorption rates of the samples were evaluated using the slope (dnW_w/dt) (Figure 3).

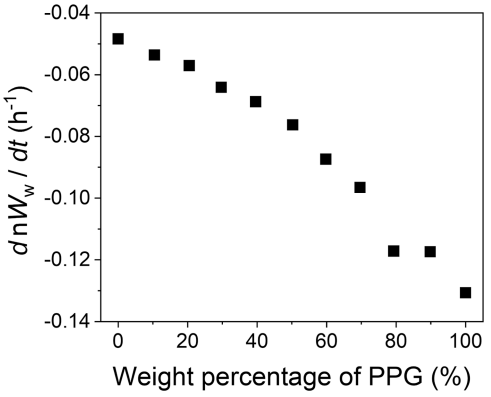

Figure 3. Slopes of the water contents with respect to the desorption time, dnW_w/dt, of PEG300 and PPG400 mixtures in different ratios, i.e., as a function of the weight percentage of PPG400 (0, 10, 20, 30, 40, 50, 60, 70, 80, 90 or 100%) in the water-desorption experiments at 20%RH and 40 °C for 4 h. Water adsorption was carried out in advance at 40%RH and 25 °C for 2 days.

Evidently, the slope decreases as the weight percentage of PPG400 increases. This indicates that the water desorption rate of the water-adsorbed molecules was improved by blending PEG300 with PPG400.

Analysis of the Mechanism of Accelerated Water Desorption by Mixing PEG300 and PPG400. The acceleration of water desorption upon mixing PEG300 and PPG400 is presumed to be largely related to the amount of water adsorbed and desorbed by PPG400, which originally had a low water-adsorption capacity and high water-desorption efficiency, owing to its poor hydrophilicity. Relevant data regarding the *n*-octanol−water partition coefficient (log P_{ow}) can be found in the safety data sheets. For PEG300, log P_{ow} is listed as −0.698 at 30 °C, and for PPG400, log P_{ow} ranges from 0.3 to 0.9 at 23 °C.[17,18] To confirm whether the addition of PPG400 enhanced water desorption in PEG300, PPG400 dried at 20%RH and 40 °C was mixed with PEG300 that had

https://doi.org/10.1021/acsomega.3c07310
ACS Omega 2024, 9, 1084−1091

fully adsorbed water at 40%RH and 25 °C, and the water desorption efficiencies of the PEG300 and PPG400 mixtures were evaluated. Comparing the water desorption efficiencies of the samples, as shown in Figure 2, the water desorption efficiency increased as the proportion of dried PPG400 increased (Figure 4, black dots). This indicates that the

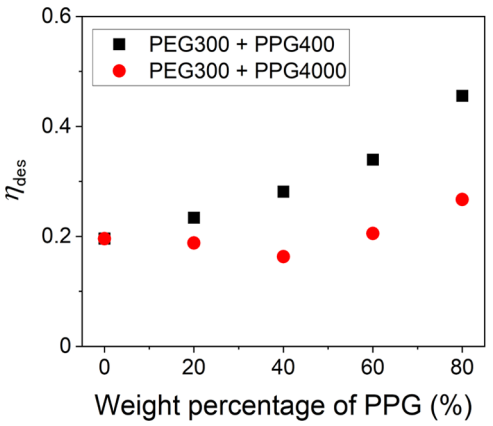

Figure 4. Water desorption efficiencies of PEG300 (adsorbed at 40% RH and 25 °C for 2 days) and PPG400 (black, dried at 20%RH and 40 °C for 2 days) and PEG300 and PPG4000 (red, dried at 20%RH and 40 °C for 2 days) mixtures as a function of the weight percentage of PPG (0, 20, 40%, 60, or 80%). The samples were heated at 20%RH and 40 °C for 2 h.

accelerated water desorption of PEG300 in the PPG400 mixtures is not only influenced by the amount of water adsorbed on PPG400 but also by the effect of promoting the desorption of water molecules adsorbed on PEG300. In other words, the interaction between PEG300 and PPG400 promotes the desorption of water molecules adsorbed on PEG300.

TG-DTA was performed to evaluate the water desorption from a thermodynamic perspective. For PEG300 and PPG400 alone, endothermic peaks with a mass decrease derived from the desorption of adsorbed water molecules were observed in both cases, and the temperature of the endothermic peaks was 93.2 °C (PEG300, Figure S6) and 50.5 °C (PEG400, Figure S7). In contrast, the water desorption temperature of the mixture of PEG300 and PPG400 (weight percentage of PPG400 = 80%) was 46.3 °C. The mixtures exhibited a single endothermic peak without splitting into two peaks (Figure 5a). Additionally, the water desorption temperature shifted to the lower temperature as the PPG400 blend ratio increased, reaching a minimum at a PPG400 weight percentage of 80% (Figure 5b).

This result is consistent with the trend of the water desorption efficiency shown in Figure 2, indicating an optimal composition (i.e., 80 wt % PPG400) in the PEG300-PPG400 mixture that maximizes the water desorption efficiency.

To confirm the water transfer between PEG300 and PPG400, a droplet of PEG300 with fully adsorbed water molecules at 40%RH and 25 °C was added onto dried PPG400 on an ATR crystal, and the change in the FT-IR spectrum of PPG400 was examined (Figure S8). Focusing on the appearance of the peak (1640 cm^{-1}) originating from the bending vibration of water, no peak originating from the bending vibration of water appeared in the FT-IR spectrum of PPG400 in the dry state, whereas immediately after the

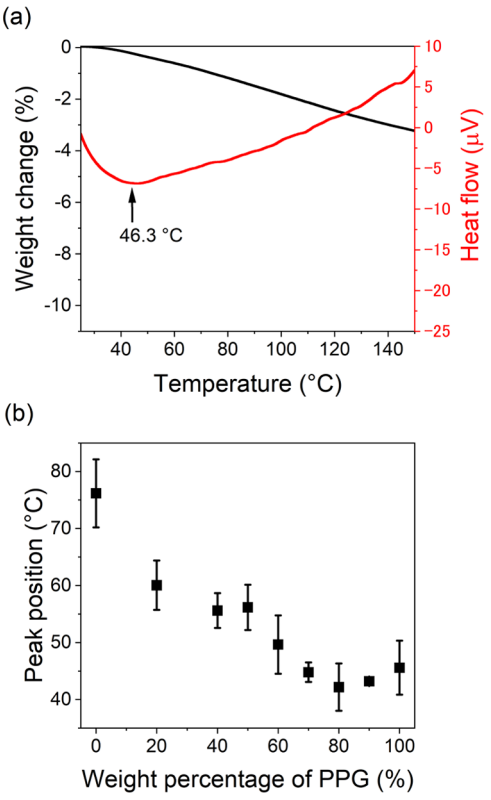

Figure 5. (a) TG-DTA curves of the water-adsorbed mixture of PEG300 and PPG400 (at 80 wt % of PPG400). Water adsorption was carried out at 40%RH and 25 °C. (b) Peak positions of the DTA curves of the water-adsorbed PEG300-PPG400 mixtures as a function of the weight percentage of PPG400. Water adsorption was carried out at 40%RH and 25 °C for 2 days.

addition of PEG300, the peak shape of PPG400 is shown in Figure S4 was maintained; however, peaks originating from the bending vibration of water molecules appeared (indicated by the arrow in Figure 6).

This indicated that the water molecules adsorbed on PEG300 were transferred to PPG400. This was due to the adsorption equilibrium of water molecules between PEG300 and PPG400, and it appeared that the desorption of water

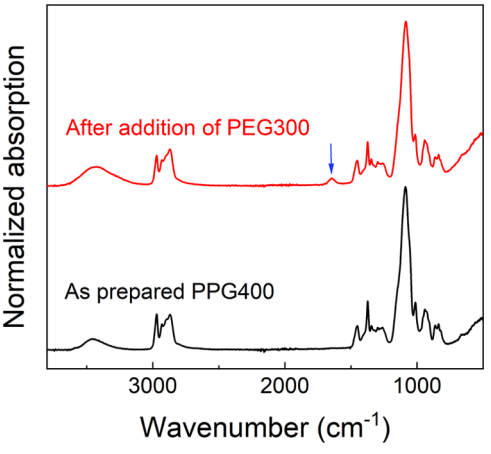

Figure 6. FT-IR spectra of dried PPG400 (black) and of PPG400 after the addition of water-adsorbed (40%RH and 25 °C for 2 days) PEG300 (red).

https://doi.org/10.1021/acsomega.3c07310
ACS Omega 2024, 9, 1084−1091

molecules from PEG300 was promoted by the movement of water molecules from PEG300 to PPG400 during desorption.

Comparative experiments were conducted with mixtures of PEG300 and PPG4000, which are less hydrophilic than the mixtures of PEG300 and PPG400, to investigate the effect of accelerated water desorption on the adsorption equilibrium. First, PPG4000 dried at 20%RH and 40 °C was mixed with PEG300, which was found to fully adsorb water at 40%RH and 25 °C. Notably, water desorption efficiencies of these mixtures did not follow a trend with increasing weight percentage of PPG4000. They were generally constant (Figure 4, red dots) and different from those of the PEG300−PPG400 mixtures. When TG-DTA was performed on the PEG300−PPG4000 mixture (at 50 wt % of PPG4000), two endothermic peaks were derived from the water desorption of PEG300 and PPG4000 (Figure S9). Furthermore, unlike that of PPG400, the IR spectrum of dried PPG4000 did not change with the addition of water-adsorbed PEG300 (Figure S10).

From the above comparative experiments of the PEG300−PPG400 and PEG300−PPG4000 mixtures, the single endothermic peak in the TG-DTA of the PEG300−PPG400 mixture shown in Figure 5a indicates that PEG300 and PPG400 interact with each other during water desorption. In other words, it can be assumed that PEG300 and PPG400 do not desorb water molecules independently. However, the adsorption equilibrium of water molecules between PEG300 and PPG400 facilitates the adsorption and desorption of water by transporting water molecules from PEG300 to PPG400. In contrast to the behavior observed in the mixture of PEG300 and PPG400, the endothermic peak in the mixture of PEG300 and PPG4000 separated into two, indicating that the PEG300 and PPG4000 mixtures did not interact and water desorption was not promoted. In other words, the level of hydrophilicity in the hydrophobic molecules within the mixture plays a significant role in determining the interaction of PEG300 with the hydrophobic molecule and the subsequent enhancement of water desorption. Since PPG400 possesses hydrophilic characteristics resembling those of PEG300, the two compounds are able to interact, thereby accelerating the desorption of water molecules from PEG300.

To clarify the cause of accelerated water desorption by mixing PPG400, ATR FT-IR measurements were performed, and it is known that the peak position of the water bending mode by IR absorption change correlates with the bonding strength of the water molecular network.[15] In the IR absorption of samples with adsorbed water molecules at 40% RH, the peak position of the water bending mode shifted to the lower wavenumber side as the mixing ratio of PPG400 increased, indicating that the intermolecular bonds between water molecules were weakened by the mixing of PPG400 (Figure 7).

It was found that the weakening of the intermolecular bonds between water molecules increased the water desorption efficiency and water desorption rate through the cooperative process of H_2O−PEG300−PPG400 interaction. In short, the temperature decrease at the endothermic peak position in DTA was caused by the weakening of the intermolecular bonds between water molecules owing to the mixing of PPG400.

Based on these results, we stipulate that the accelerated water desorption in mixtures of PEG300 and PPG400 is governed by mechanisms illustrated in Figure 8.

The improved water desorption efficiency achieved by mixing PPG400, as shown in (Figure 2), was due to the water

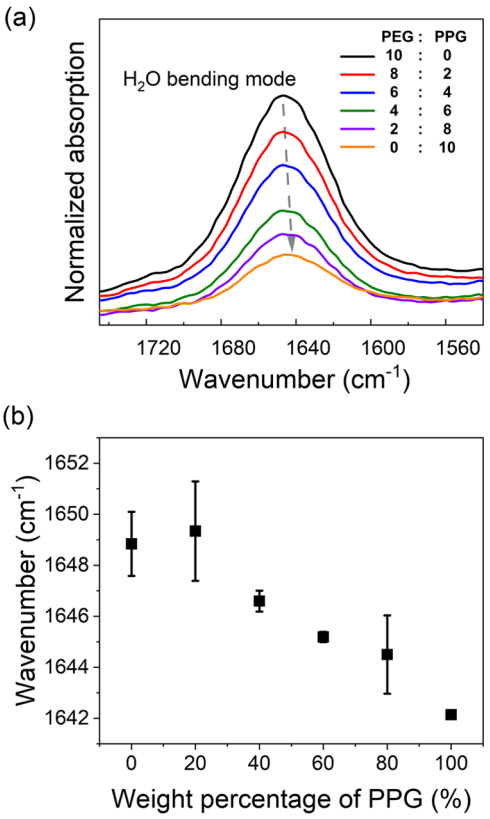

Figure 7. (a) FT-IR spectra of water-adsorbed PEG300 and PPG400 mixtures (the weight percentage of PPG400 is 0% (black), 20% (red), 40% (blue), 60% (green), 80% (purple), or 100% (orange). Water adsorption was carried out at 40%RH and 25 °C for 2 days). (b) Peak center of gravity position of the H2O bending mode. PEG300 and PPG400 were mixed in various ratios. Water adsorption was carried out at 40%RH and 25 °C for 2 days.

adsorption or desorption capacity of PPG400 and the adsorption equilibrium of water molecules between PEG300 and PPG400. First, PPG400 is more hydrophobic than PEG300 and therefore more efficient in water desorption by nature. This is evident from the difference in the endothermic peak temperatures of DTA in Figures S6 and S7. Therefore, as the weight percentage of PPG400 increased, the water-desorption efficiency of the mixture increased. However, the effect of accelerated water desorption was not solely due to the differences in the water adsorption or desorption capacities of PEG300 and PPG400. Because PPG400 is sufficiently hydrophilic, water molecules were exchanged with PEG300. Specifically, the mechanism of accelerated water desorption is as follows: Water molecules adsorbed on PEG300 and PPG400 preferentially desorb from the water molecules bound to PPG400, which is more hydrophobic. Subsequently, the water molecules adsorbed on PEG300 were transferred to PPG400 to compensate for the water molecules desorbed from PPG400. Because the two factors described above increased the water desorption efficiency, the water desorption efficiency shown in Figure 2 was higher than that of PPG400 alone at PPG400 weight percentages of 70−80% and was the highest at 80%.

The water desorption efficiency of the present work (PEG300 and PPG400 mixtures, the weight percentage of PPG400 was 80%) was compared with that of solid adsorbents, such as metal−organic frameworks (MOFs), and liquid

https://doi.org/10.1021/acsomega.3c07310
ACS Omega 2024, 9, 1084−1091

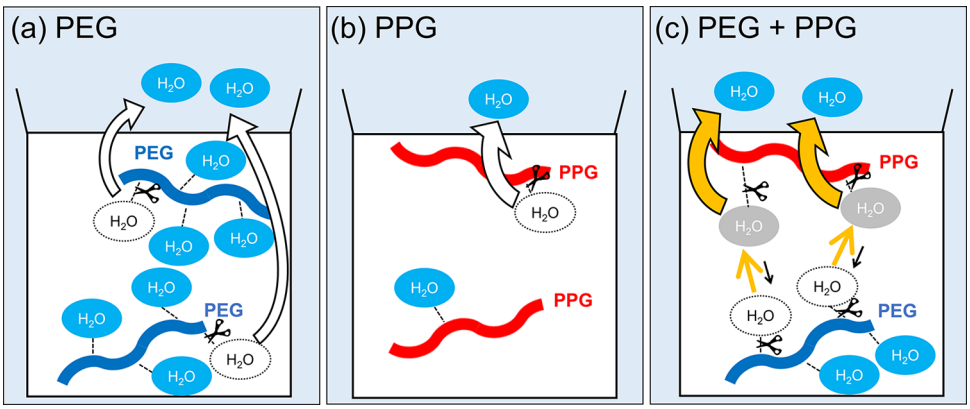

Figure 8. Schematic illustration of proposed water desorption mechanisms in PEG300 (a), PPG400 (b), and PEG300 and PPG400 mixtures (c).

adsorbents, such as metal-salt solutions, ionic liquids, and their composite systems (Figure 9).[14,19−27]

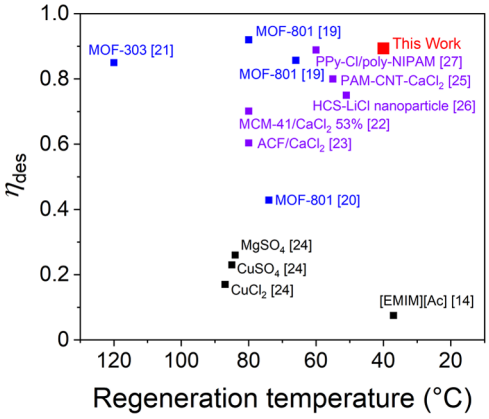

Figure 9. Comparison with the reported values for desorption efficiency and regeneration temperature: this study (mixture of PEG300 and 80 wt % PPG400) (red), metal−organic frameworks (blue),[19−21] liquid sorbents (black),[14,24] and composites (purple).[22,23,25−27] Numbers in square brackets indicate reference numbers.

Overall, these results show that the water adsorbent formulated here exhibited a high water desorption efficiency at low regeneration temperatures. This indicates that liquid-based water adsorbents with partially hydrophobic components can recover most adsorbed water under mild conditions. Therefore, the partial mixing of hydrophobic molecules with liquid adsorbents is a promising approach for developing liquid adsorbents for DAC and AWH with high energy efficiency.

CONCLUSIONS

In the present study, PEG300 and PPG400, which have different hydrophilicities, were mixed to increase the desorption efficiency of the adsorbed water molecules. PPG400 with moderately low hydrophilicity interacted with PEG300, improving the water desorption efficiency. The accelerated water desorption factor is the adsorption equilibrium of water molecules between those of PEG300 and PPG400. The higher the blending ratio of PPG400, the higher the water desorption efficiency, with the highest value when the weight percentage of PPG400 was 80% at 40 °C. It should be emphasized that the PEG300/PPG400 mixtures have low desorption temperatures close to the atmospheric temperature and high desorption efficiency. This value showed the lowest regeneration temperature and the highest water desorption efficiency compared to those in previous studies. However, at this stage, we have not yet determined the conditions under which mixing hydrophobic molecules increases the net water recovery. In the future, it is expected that a similar water desorption mechanism will be incorporated into various hygroscopic liquids to develop more energy-efficient liquid adsorbents for DAC and AWH, which will compensate for the disadvantages of liquid adsorbents in terms of their high energy barriers during water desorption.

ASSOCIATED CONTENT

Supporting Information

The Supporting Information is available free of charge at https://pubs.acs.org/doi/10.1021/acsomega.3c07310.

Experimental setup for the water adsorption and desorption experiments (Figure S1); flowchart of the experimental procedure (Figure S2); FT-IR spectra of PEG300 before and after water adsorption (Figure S3); FT-IR spectra of PPG400 before and after water adsorption (Figure S4); water contents of PEG300 and PPG400 mixtures as a function of time, represented by a semi-logarithmic plot in water desorption experiments (Figure S5); TG-DTA curves of water-adsorbed PEG300 (Figure S6); TG-DTA curves of water-adsorbed PPG400 (Figure S7); schematic illustration of the ATR experiment for evaluating water penetration into dried PPG (Figure S8); TG-DTA curves of water-adsorbed mixture of PEG300-PPG4000 (Figure S9); FT-IR spectra of dried PPG4000 and of PPG4000 after addition of water-adsorbed PEG300 (Figure S10) (PDF)

AUTHOR INFORMATION

Corresponding Authors

Arisa Fukatsu − *Department of Materials Science, Graduate School of Engineering, Osaka Metropolitan University, Sakai, Osaka 599-8531, Japan;* orcid.org/0000-0002-2887-1452; Email: fukatsu@omu.ac.jp

Masahide Takahashi − *Department of Materials Science, Graduate School of Engineering, Osaka Metropolitan University, Sakai, Osaka 599-8531, Japan;* orcid.org/0000-0001-7273-1660; Email: masa@omu.ac.jp

https://doi.org/10.1021/acsomega.3c07310
ACS Omega 2024, 9, 1084−1091

Authors

Daisuke Ikegawa − *Department of Materials Science, Graduate School of Engineering, Osaka Metropolitan University, Sakai, Osaka 599-8531, Japan*

Kenji Okada − *Department of Materials Science, Graduate School of Engineering, Osaka Metropolitan University, Sakai, Osaka 599-8531, Japan;* orcid.org/0000-0003-2176-693X

Complete contact information is available at: https://pubs.acs.org/10.1021/acsomega.3c07310

Author Contributions

D.I. contributed to experiments, validation, and writing−original draft; A.F. contributed to design of methodology, curation, resources, validation, writing−review and editing, and funding acquisition; K.O. contributed to validation, resources, and writing−review and editing; M.T. contributed to design of methodology, validation, resources, writing−review and editing, and funding acquisition.

Funding

This work was partially supported by grand-in-aid from the Ministry of Education, Culture, Sports, Science, and Technology (MEXT), administrated by the Japan Society for the Promotion of Science (JSPS) (JSPS KAKENHI Grant Numbers JP20H00401 and JP22K14492), Izumi Science and Technology Foundation, Kansai Research Foundation for Technology Promotion, and Nippon Sheet Glass Foundation for Materials Science and Engineering.

Notes

The authors declare no competing financial interest.

■ ACKNOWLEDGMENTS

This work was partially supported by grand-in-aid from the Ministry of Education, Culture, Sports, Science, and Technology (MEXT), administrated by the Japan Society for the Promotion of Science (JSPS) (JSPS KAKENHI Grant Numbers JP20H00401 and JP22K14492), Izumi Science and Technology Foundation, Kansai Research Foundation for Technology Promotion, and Nippon Sheet Glass Foundation for Materials Science and Engineering.

■ ABBREVIATIONS

DAC, desiccant air conditioning; AWH, atmospheric water harvesting; PEG, poly(ethylene glycol); PPG, poly(propylene glycol); TG-DTA, thermogravimetry-differential thermal analysis; [EMIM][Ac], 1-ethyl-3-methylimidazolium acetate; ATR, attenuated total reflection; FT-IR, Fourier-transform infrared; MOF, metal−organic framework; W_w, water content; M_s, weight of sample; M_s°, initial weight of sample; η_{des}, water desorption efficiency; W_{des}, amount of water desorbed; W_{ads}, amount of water adsorbed; nW_w, normalized water content; $\log P_{ow}$, *n*-octanol−water partition coefficient

■ REFERENCES

(1) Moodley, P.Sustainable Biofuels: Opportunities and Challenges. In *Sustainable Biofuels*; Elsevier, 2021; pp 1−20.

(2) Yu, B.; Duan, J.; Cong, H.; Xie, W.; Liu, R.; Zhuang, X.; Wang, H.; Qi, B.; Xu, M.; Wang, Z. L.; Zhou, J. Thermosensitive Crystallization-Boosted Liquid Thermocells for Low-Grade Heat Harvesting. *Science* **2020**, *370* (6514), 342.

(3) Forman, C.; Muritala, I. K.; Pardemann, R.; Meyer, B. Estimating the Global Waste Heat Potential. *Renewable Sustainable Energy Rev.* **2016**, *57*, 1568.

(4) Cullen, J. M.; Allwood, J. M. Theoretical Efficiency Limits for Energy Conversion Devices. *Energy* **2010**, *35* (5), 2059.

(5) Xu, A.; Xu, M.; Xie, N.; Liang, J.; Zeng, K.; Kou, G.; Liu, Z.; Yang, S. Performance Analysis of a Cascade Lithium Bromide Absorption Refrigeration/Dehumidification Process Driven by Low-Grade Waste Heat for Hot Summer and Cold Winter Climate Area in China. *Energy Convers. Manag.* **2021**, *228*, No. 113664.

(6) Li, R.; Wang, W.; Shi, Y.; Wang, C. T.; Wang, P. Advanced Material Design and Engineering for Water-Based Evaporative Cooling. *Adv. Mater.* **2023**, No. e2209460.

(7) Miernicki, E. A.; Heald, A. L.; Huff, K. D.; Brooks, C. S.; Margenot, A. J. Nuclear Waste Heat Use in Agriculture: History and Opportunities in the United States. *J. Cleaner Prod.* **2020**, *267*, No. 121918.

(8) Santosh, R.; Lee, H.-S.; Kim, Y.-D. A Comprehensive Review on Humidifiers and Dehumidifiers in Solar and Low-Grade waste Heat Powered humidification-Dehumidification Desalination Systems. *J. Cleaner Prod.* **2022**, *347*, No. 131300.

(9) Abdelgaied, M.; Saber, M. A.; Bassuoni, M. M.; Khaira, A. M. Adsorption Air Conditioning: A Comprehensive Review in Desiccant Materials, System Progress, and Recent Studies on Different Configurations of Hybrid Solid Desiccant Air Conditioning Systems. *Environ. Sci. Pollut. Res.* **2023**, *30* (11), 28344.

(10) Lu, H.; Shi, W.; Guo, Y.; Guan, W.; Lei, C.; Yu, G. Materials Engineering for Atmospheric Water Harvesting: Progress and Perspectives. *Adv. Mater.* **2022**, *34* (12), No. e2110079.

(11) Li, X.-W.; Zhang, X.-S.; Quan, S. Single-Stage and Double-Stage Photovoltaic Driven Regeneration for Liquid Desiccant Cooling System. *Appl. Energy* **2011**, *88* (12), 4908.

(12) Che, C.; Cheng, X.; Tong, S.; Yin, Y. Deep Utilization of Low-Grade Heat Through Compositional Modulation of Multi-Component Liquid Desiccant. *ACS Appl. Mater. Interfaces* **2022**, *14* (31), 35581.

(13) Wang, X.; Li, X.; Liu, G.; Li, J.; Hu, X.; Xu, N.; Zhao, W.; Zhu, B.; Zhu, J. An Interfacial Solar Heating Assisted Liquid Sorbent Atmospheric Water Generator. *Angew. Chem., Int. Ed.* **2019**, *58* (35), 12054.

(14) Qi, H.; Wei, T.; Zhao, W.; Zhu, B.; Liu, G.; Wang, P.; Lin, Z.; Wang, X.; Li, X.; Zhang, X.; Zhu, J. An Interfacial Solar-Driven Atmospheric Water Generator Based on a Liquid Sorbent With Simultaneous Adsorption-Desorption. *Adv. Mater.* **2019**, *31* (43), No. e1903378.

(15) Seki, T.; Chiang, K. Y.; Yu, C. C.; Yu, X.; Okuno, M.; Hunger, J.; Nagata, Y.; Bonn, M. The Bending Mode of Water: A Powerful Probe for Hydrogen Bond Structure of Aqueous Systems. *J. Phys. Chem. Lett.* **2020**, *11* (19), 8459.

(16) Patlakas, P.; Stathopoulos, C.; Flocas, H.; Kalogeri, C.; Kallos, G. Regional Climatic Features of the Arabian Peninsula. *Atmosphere* **2019**, *10* (4), 220.

(17) Polyethylene glycol 300 EMPROVE ESSENTIAL Ph Eur, CAS RN: 25322−68−3; Millipore- 8.17002; Version 8.9; Version 8.9, United States, July 5, 2022. https://www.emdmillipore.com/US/en/product/msds/MDA_CHEM-817002.

(18) Poly(propylene glycol), CAS RN: 25322−69−4, Aldrich-202304; Version 6.4; Sigma-Aldrich Inc., United States, Jun 7, 2021. https://www.sigmaaldrich.com/US/en/sds/aldrich/202304.

(19) Kim, H.; Yang, S.; Rao, S. R.; Narayanan, S.; Kapustin, E. A.; Furukawa, H.; Umans, A. S.; Yaghi, O. M.; Wang, E. N. Water Harvesting From Air With Metal-Organic Frameworks Powered by Natural Sunlight. *Science.* **2017**, *356* (6336), 430.

(20) Kim, H.; Rao, S. R.; Kapustin, E. A.; Zhao, L.; Yang, S.; Yaghi, O. M.; Wang, E. N. Adsorption-Based Atmospheric Water Harvesting Device for Arid Climates. *Nat. Commun.* **2018**, *9* (1), No. 1191.

(21) Hanikel, N.; Prévot, M. S.; Fathieh, F.; Kapustin, E. A.; Lyu, H.; Wang, H.; Diercks, N. J.; Glover, T. G.; Yaghi, O. M. Rapid Cycling and Exceptional Yield in a Metal-Organic Framework Water Harvester. *ACS Cent. Sci.* **2019**, *5* (10), 1699.

(22) Ji, J. G.; Wang, R. Z.; Li, L. X. New Composite Adsorbent for Solar-Driven Fresh Water Production From the Atmosphere. *Desalination* **2007**, *212* (1−3), 176.
(23) Wang, J. Y.; Liu, J. Y.; Wang, R. Z.; Wang, L. W. Experimental Investigation on Two Solar-Driven Sorption Based Devices to Extract Fresh Water from Atmosphere. *Appl. Therm. Eng.* **2017**, *127*, 1608.
(24) Li, R.; Shi, Y.; Shi, L.; Alsaedi, M.; Wang, P. Harvesting Water From Air: Using Anhydrous Salt With Sunlight. *Environ. Sci. Technol.* **2018**, *52* (9), 5398.
(25) Li, R.; Shi, Y.; Alsaedi, M.; Wu, M.; Shi, L.; Wang, P. Hybrid Hydrogel With High Water Vapor Harvesting Capacity for Deployable Solar-Driven Atmospheric Water Generator. *Environ. Sci. Technol.* **2018**, *52* (19), 11367.
(26) Li, R.; Shi, Y.; Wu, M.; Hong, S.; Wang, P. Improving Atmospheric Water Production Yield: Enabling Multiple Water Harvesting Cycles With Nano Sorbent. *Nano Energy* **2020**, *67*, No. 104255.
(27) Zhao, F.; Zhou, X.; Liu, Y.; Shi, Y.; Dai, Y.; Yu, G. Super Moisture-Absorbent Gels for All-Weather Atmospheric Water Harvesting. *Adv. Mater.* **2019**, *31* (10), No. e1806446.

https://doi.org/10.1021/acsomega.3c07310
ACS Omega 2024, 9, 1084−1091